

UC Irvine

UC Irvine Previously Published Works

Title

Multivariate pattern analysis of the human pSTS: A comparison of three prototypical localizers

Permalink

<https://escholarship.org/uc/item/9zj5v95w>

Authors

Dasgupta, Samhita

Srinivasan, Ramesh

Grossman, Emily D

Publication Date

2018-11-01

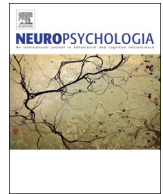
DOI

10.1016/j.neuropsychologia.2018.10.004

Copyright Information

This work is made available under the terms of a Creative Commons Attribution License, available at <https://creativecommons.org/licenses/by/4.0/>

Peer reviewed



Multivariate pattern analysis of the human pSTS: A comparison of three prototypical localizers

Samhita Dasgupta, Ramesh Srinivasan, Emily D. Grossman*

Department of Cognitive Sciences, University of California Irvine, United States

ARTICLE INFO

Keywords:

Biological motion perception
Face perception
Social understanding
Posterior superior temporal sulcus
Functional magnetic resonance imaging

ABSTRACT

The posterior extent of the human superior temporal sulcus (pSTS) is an important cortical region for detecting animacy, attributing agency to others, and decoding goal-directed behavior. Theoretical accounts attribute these cognitive skills to unique neural populations that have been difficult to identify empirically (Hein and Knight, 2008). The aim of this study is to evaluate the multivariate statistical structure of pSTS activation patterns when viewing different social cues. We identified a core conjunction region on pSTS from univariate responses with preference for point-light biological motion, faces and the attribution of social concepts to simple animated shapes. In a multivariate analysis, we characterized the similarity structure of the resulting activation patterns after controlling for variance in the activation profile elicited by form and motion features. We found strong antagonistic activation profiles between the social conditions and their localizer controls, a harbinger of why these canonical localizers are so effective, even in individual subjects. We also found unique patterns of similarity between the three core social conditions. Our findings are consistent with the Shultz et al. (2015) model of pSTS function in which separate neural populations exist for animacy detection from body parts versus for extracting intentional cues from movement.

1. Introduction

Interacting with other individuals relies on a number of perceptual and cognitive mechanisms, including decoding gaze and actions, so as to build internal representations of intentions and mental states. These complex processes are broadly within the scope of social perception and cognition, and are linked to cortical activity on the posterior superior temporal sulcus (pSTS; Puce and Perrett, 2003; Pyles and Grossman, 2013; Dziura and Thompson, 2014; Yang et al., 2015).

The field has long hypothesized the STS to host domain-specific modules specialized for processing social cues, including neural populations that encode changeable aspects of faces (e.g. eye gaze and emotional expression; Puce et al., 1998; Hoffman and Haxby, 2000; Haxby et al., 2000; Grossman and Blake, 2002) and that decode actions for recognition (Grossman et al., 2000; Beauchamp et al., 2002; Jastorff and Orban, 2009). The STS is also linked to the attribution of agency when viewing animations that signal animacy even without the presence of body parts (Castelli et al., 2000; Martin and Weisberg, 2003; Gao et al., 2012). All of these neural populations are believed to support the broader cognitive task of mentalizing, itself linked to the more dorsal temporoparietal junction (TPJ; Gallagher & Frith, 2003; Saxe and Wexler, 2005; Carter and Huettel, 2013).

Isolating the neural signals associated uniquely with these putative modules, however, has proven difficult. Univariate and meta-analytic approaches yield complex patterns of activation that overlap between different combinations of social perceptual tasks (e.g. Saxe et al., 2009; Bahnmann et al., 2010; Hein and Knight, 2008; Van Overwalle, 2009; Carter and Huettel, 2013; Grosbras et al., 2012; Lahnakoski et al., 2012). For example, within-subject univariate mapping reveals spatially complex and overlapping maps of activation between biological motion perception and viewing Heider-Simmel like animations (Gobbini et al., 2007), and between biological motion and face perception (Grossman and Blake, 2002; Engell and McCarthy, 2013; Deen et al., 2015).

Multivariate approaches, however, suggest a more promising means for separating the underlying neural populations. For example, face recognition and point-light biological motion can be dissociated from overlapping or adjacent ROIs when analyzing the pattern response (Deen et al., 2015; Isik et al., 2017). Likewise, more dorsally in the TPJ, the multivariate BOLD activity dissociates neural activity when viewing point-light biological motion from engaging theory of mind as assessed through false-belief short stories, and from the neural signals linked to attentive reorienting (Lee and McCarthy, 2014).

We hypothesize that spatial variations in the pSTS voxel pattern

* Correspondence to: Department of Cognitive Sciences, University of California Irvine, 3151 Social Science Plaza, Irvine, CA 92697-5100, United States.
E-mail address: grossman@uci.edu (E.D. Grossman).

may provide evidence for unique, or shared, neural representations for encoding social cues on the STS. Therefore, in this study we evaluate the multivariate similarity of the voxel patterns from a single conjunction pSTS region of interest. We compare these activation patterns elicited by three localizers commonly used in the field of social perception: biological motion perception, face perception, and social understanding from Heider-Simmel like animations (e.g. Grossman et al., 2000; Hoffman and Haxby, 2000; Martin and Weisberg, 2003). We note that these localizers all have high sensitivity for isolating the pSTS despite the unique perceptual features and cognitive tasks imposed by each.

To characterize the underlying similarity structure, we subjected the conjunction pSTS to a multivariate correlation analysis of similarity using partial correlations, which identifies variance unique to any two tasks and not shared with other tasks included in the model (Salvador et al., 2005; Marrelec et al., 2006). This approach is particularly helpful for removing redundant variance due to mixing of neural populations in the individual voxel responses, anticipated from previous work showing significant overlap in peak responses among conditions like these (Deen et al., 2015). Moreover, the partial correlation approach is effective for controlling nuisance factors epiphenomenal to the variables of interest (e.g. task confounds, partial volume effects, and subject motion) that may artificially inflate marginal correlation scores. In this approach, we applied the technique to remove spatial variance driven by form and motion features not specific to the social cues. The results from this analysis distinguish between two dominant models of functional specialization of the pSTS.

2. Methods

2.1. Participants

A total of sixteen individuals (eight male) from the UC Irvine campus and community participated in this experiment. Subjects completed two identical scanning sessions on two separate days. The Human Protections Review Board at the University of California Irvine approved all recruiting and consent procedures.

2.2. Localizers

Subjects participated in three social localizer tasks and two non-social control localizers (described below; Fig. 1). The social localizers were chosen because of their strength in identifying the pSTS and other brain regions associated with social perception and cognition. The nonsocial localizer conditions were selected to statistically control for the presence of motion and form contours in the different scan conditions.

The localizer scans were ordered pseudorandomly, with four scans of each localizer collected over two scanning sessions (two scans of each localizer collected within each scanning session). All stimuli were displayed using Psychophysics Toolbox (Brainard, 1997; Pelli, 1997) in Matlab (Mathworks, Inc.).

2.2.1. Biological motion (BioMotion)

Point-light biological motion animations depicting 25 unique actions were constructed using 13 black dots (0.17° of visual angle) representing the major joints and head of an actor (Grossman et al., 2000). The overall figure subtended approximately $8 \times 3.5^\circ$ of visual angle and was positioned at the center of the screen. Scrambled motion was constructed by randomizing the spatial location of the starting position dots while leaving the motion vectors intact. Blocks consisted of 10 one-second animations with a 600 ms inter-stimulus interval. Subjects performed a 1-back task (report a repeated animation) on each stimulus, with an average of 3 repeats within each block. Each scan consisted of six alternating biological motion and scrambled blocks, separated by a 4 s fixation interval. Subjects participated in four

biological motion localizer scans, for a total of 24 blocks per condition.

2.2.2. Face perception (Faces)

The face perception localizer was constructed similar to Hoffman and Haxby (2000). Stationary grayscale images of faces ($7.5 \times 3^\circ$ visual angle) were obtained from the Radboud database (Langner et al., 2010), with all faces depicting adults in the frontal view with gaze directed to the left, right or straight ahead, with happy, sad, angry, disgusted or neutral emotional expression. Scrambled faces were created from the face images by pixel scrambling them in units of 0.36° visual angle. Each 16 s block contained ten 750 ms images separated by 1000 ms interstimulus interval. During the face blocks, subjects were cued to perform a 1-back task on the actor's identity (irrespective of facial expression or gaze direction) or gaze direction (irrespective of facial expression or identity) with five repeats per block (on average). Each scan consisted of six alternating face task and scrambled blocks, separated by a 4 s fixation interval. Subjects participated in four face localizer scans, for a total of 24 blocks per condition.

2.2.3. Social animations (Social)

The social cognition localizer was adapted from Martin and Weisberg (2003), with stimuli generously provided by Alex Martin. Subjects viewed 21 s video vignettes, similar to those developed by Heider-Simmel (1944). These sequences depicted geometric shapes moving such that they readily appeared as agents (self-motivated actors) engaged in social interactions, or as components of moving mechanical objects. Each vignette was immediately followed by a 6 s response window with a multiple choice selection in which subjects selected one of four phrases that best described the preceding scene. Blocks in the social cognition localizer were 27 s long, separated by a 3 s interblock interval, for a total of 8 blocks/scan. Subjects participated in four social cognition localizer scans, for a total of 16 blocks per condition.

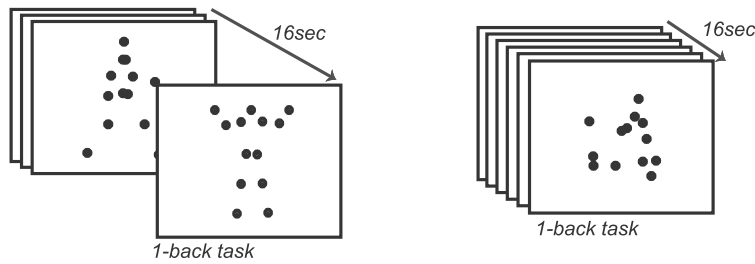
2.2.4. Optic flow (OpFlow)

To isolate activation patterns linked to motion perception (without social interpretation), we collected brain responses using an optic flow localizer similar to Morrone et al. (2000). Subjects viewed expanding and contracting optic flow random dot patterns constructed from 500 dots moving with an average speed of $8.5^\circ/s$ randomly distributed within an 8.7° circular aperture. Throughout the 16 s blocks of motion, the direction of contraction and expansion randomly alternated to minimize the buildup of visual motion aftereffects. Subjects passively viewed the stimulus, with no task other than to remain fixated on the central fixation cross and maintain attention on the stimulus. Each scan consisted of six alternating 16 s optic flow and stationary blocks, separated by a 3 s fixation interval. Subjects participated in four optic flow localizer scans, for a total of 24 blocks per condition.

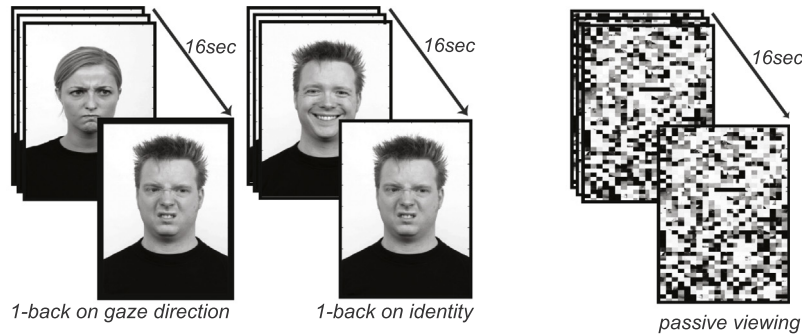
2.2.5. Object perception (Object)

To isolate activation patterns associated with viewing object forms (without social interpretation), we collected brain responses using an object localizer similar to Grill-Spector et al. (2001). Subjects viewed grayscale stationary images ($8 \times 3.5^\circ$ of visual angle) of common household objects (e.g. spoon, cup, comb, food, chair). Scrambled versions of the same images were constructed by scrambling the Fourier phase components of the original images. Each 16 s block contained 10 one sec images separated by 600 ms interstimulus interval. During the object blocks, subjects were cued to perform a 1-back task on each item within the block with an average of 3 repeats within each block. Each scan consisted of six alternating object and scrambled blocks, separated by a 4 s fixation interval. Subjects participated in four object localizer scans, for a total of 24 blocks per condition.

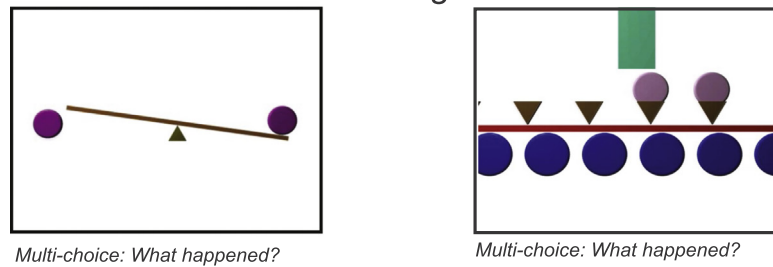
A. Biological vs Scrambled motion



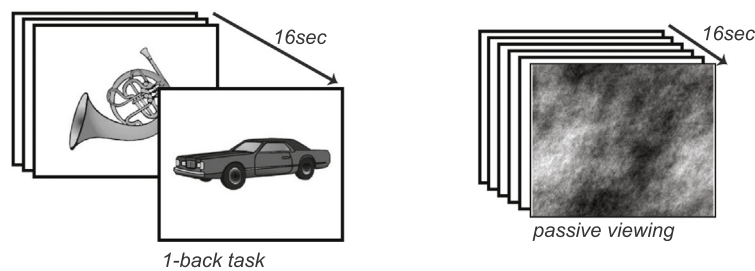
B. Faces vs scrambled faces



C. Social vs mechanical vignettes



D. Common vs phase scrambled objects



E. Optic flow vs stationary dots

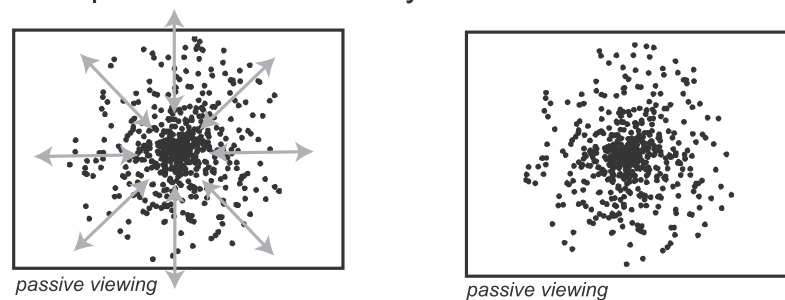


Fig. 1. Schematic of stimuli used in the three core social cognitive localizers and two non-social control localizers. A. Point-light biological (left) and scrambled (right) motion. B. Face and gaze recognition (left) and pixel scrambled images (right). C. Vignettes of social interactions (left) and mechanical devices (right). D. Object recognition (left) and phase scrambled images (right). E. Motion control, with optic flow (left) and static dot pattern (right).

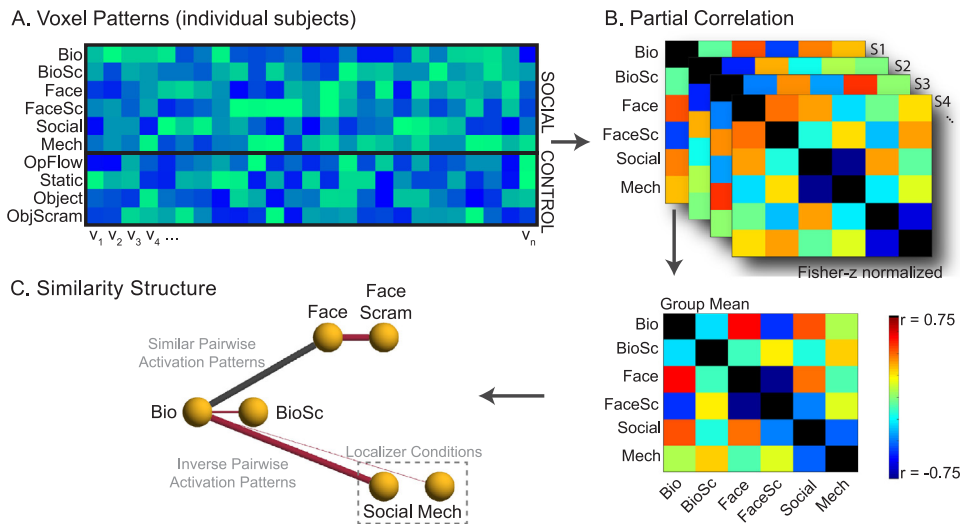


Fig. 2. Schematic of analysis pipeline and interpretation of graphical models. (A) The voxel-wise spatial pattern in conjunction pSTS identified in the individual subjects is computed from the peak block responses for each condition. Three social conditions and their localizer controls serve as the conditions of interest (social conditions). Optic flow and object localizers serve as nonsocial control activation patterns. (B) The spatial patterns are then subjected to a partial correlation analysis that controls for the activation patterns generated by the four non-social control conditions. This analysis, computed on individual subjects, returns the pairwise similarity structure of the six social conditions of interest. These correlation scores are Fisher r -z normalized and averaged into a group similarity matrix. (C) Graphical model of a hypothetical similarity structure. Conditions of interest are shown as nodes and statistically significant similarity

scores are shown as edges. All edges denote variance shared by the two connected conditions that is not explained by variance observed in any other condition. Significance is assessed as the correlation strengths that exceed 99% two-tailed confidence intervals computed on a null distribution. Edge color indicates the direction of the correlation (black: positive, red: negative) and edge thickness indicates strength of the correlation. (For interpretation of the references to color in this figure legend, the reader is referred to the web version of this article.)

2.3. Imaging

MR images were collected on the Philips Achieva 3T scanner equipped with an 8-channel phased array head coil, housed in the UCI Research Imaging Center. High-resolution anatomical images were acquired for each individual (T1-weighted MPRAGE, TE = 3.7 ms, flip angle = 8°, 200 sagittal slices, 256 × 256 matrix, 1 × 1 × 1 mm³ voxels). Functional images were collected for the whole brain using single-shot, T2*-weighted gradient EPI imaging (voxel size 2.0 × 2.0 × 4.0 mm³, TE = 30 ms, flip angle = 90 deg, A-P phase encoding, 32 axial slices acquired interleaved with 0 mm gap between slices, SENSE factor = 2, TR = 2000 ms, 128 volumes per scan). Stimuli were projected using a Christie DLV 1400-DX DLP projector aimed through a waveguide onto a custom projector screen mounted at the head of the scanner. Subjects viewed the animations through a periscope mirror and responses were collected on an MR-compatible button box (Current Designs, Inc.).

2.4. Analysis

Functional images were corrected for motion within and across scans, mean intensity corrected, co-registered to the individual subject high-resolution anatomical images, and resampled into 2 × 2 × 2 mm voxels when transformed into standardized Talairach space. All of these preprocessing steps were conducted using BrainVoyager QX (Brain Innovations, Inc.).

To avoid any possible concern of circularity, we conducted a split-half analysis in which independent data was used for the localization of the conjunction pSTS and the multivariate pattern analysis. Subjects participated in four scans for each localizer, which were divided into odds (scans 1 and 3) and evens (scans 2 and 4). We used the odd scans to identify the pSTS region of interest (the conjunction analysis), and the even scans to calculate the similarity patterns (multivariate analysis). Both analyses were conducted on individual subjects in volumetric space.

2.4.1. Conjunction analysis

Localizers were analyzed using hemodynamic predictors estimating the blocked responses for the two conditions included in each localizer. The point-light biological motion pSTS was identified as the region on the superior temporal sulcus that was significantly more activation by biological motion as compared to scrambled motion, as per Grossman

et al. (2000). The face-responsive pSTS region was identified as the region on the pSTS which was more activated when viewing faces as compared to scrambled faces, as per Hoffman and Haxby (2000). We note that instructions to direct attention to identify and gaze both yielded activation on the pSTS, and the contrast between these conditions was not sufficiently powerful to consistently localize the pSTS in individual subjects. We therefore collapsed across the two face attention conditions and identified a face specific (but task-invariant) pSTS region of interest. The social cognitive pSTS was identified as the region more activated when viewing social vignettes as compared to mechanical vignettes, as per Martin and Weisberg (2003).

The conjunction pSTS was mapped using a formal conjunction analysis (Nichols et al., 2005) with the planned contrast of the social conditions versus the control within each localizer. Voxels must pass significance tests for each localizer in order to survive and contribute to the conjunction ROI. Significance was assessed at a false discovery rate $q < 0.05$ (Genovese et al., 2002).

2.4.2. Multivariate analyses

All multivariate analyses were conducted in Matlab (Mathworks, Inc.) using Neuroelf (<http://neuroelf.net>) to interface with Brain Voyager file formats and built-in tools to analyze the covariance structure. The construction of the graphical models was conducted using the BrainNet Viewer toolbox (Xia et al., 2013). Procedures for the multivariate pattern analysis are shown in Fig. 2. The conjunction analyses yielded individual subject ROIs of varying sizes (see Table 1). Therefore, to control for possible variance in statistical analyses of the activation patterns due to spatial extent, we fixed the activation pattern as a sphere of 15 mm radius centered on the centroid of the individual subject Talairach coordinates. Results do not differ in analyses applied to individual (variably sized) or fixed size ROIs, and so analysis of the spherical fixed-size patterns are presented here.

For each of the localizer scans we extracted voxel patterns associated with each condition, computed from the saturated BOLD response for each block. This was extracted as the three volumes (6 s) at the peak of the BOLD response for each block, allowing a hemodynamic delay of 8–10 s following onset of the block. We then averaged the individual block estimates of the activation patterns to yield ten unique pSTS activation patterns, one for each condition (experimental and control for the five types of scans) per subject.

To compute similarity on the multivariate response, we subjected the activation patterns to a partial correlation analysis that controlled

Table 1

Mean centroid coordinates and volume of the individual subject right and left conjunction pSTS. Centroids are given in Talairach coordinates and volume is given in units of mm³.

| Sub | Left hemisphere | | | | Right hemisphere | | | |
|-----|-----------------|-------|------|-------|------------------|-------|------|-------|
| | X | Y | Z | Vol | X | Y | Z | Vol |
| 1 | -50.3 | -47.8 | 11.0 | 67.8 | 52.4 | -42.2 | 14.4 | 164.0 |
| 2 | -49.0 | -44.3 | 3.3 | 26.0 | - | - | - | - |
| 3 | -52.6 | -48.5 | 5.5 | 119.0 | 53.6 | -43.7 | 6.3 | 353.0 |
| 4 | -48.0 | -46.5 | 2.5 | 341.2 | 44.6 | -54.6 | 6.8 | 393.9 |
| 5 | -42.4 | -52.5 | 5.2 | 64.0 | 45.5 | -44.1 | 8.1 | 76.5 |
| 6 | 46.9 | -46.6 | 0.6 | 23.0 | -52.4 | -61.9 | 12.9 | 99.5 |
| 7 | -49.5 | -47.3 | 2.9 | 77.0 | 47.5 | -47.1 | 2.3 | 36.2 |
| 8 | -54.8 | -50.6 | 6.7 | 170.1 | 50.5 | -45.1 | 8.3 | 323.8 |
| 9 | -54.5 | -52.4 | 11.8 | 20.0 | 47.9 | -51.7 | 6.9 | 295.9 |
| 10 | -52.7 | -52.8 | 5.3 | 43.0 | 48.0 | -47.3 | 3.1 | 54.0 |
| 11 | -52.8 | -51.8 | 11.1 | 105.0 | 48.3 | -40.5 | 3.4 | 288.5 |
| 12 | -57.9 | -47.3 | 16.0 | 110.0 | 50.7 | -42.6 | 10.7 | 616.0 |
| 13 | -42.0 | -44.1 | 11.7 | 105.5 | 46.1 | -36.9 | 12.0 | 295.0 |
| 14 | -41.4 | -55.9 | 7.4 | 167.2 | 54.9 | -41.1 | 11.5 | 518.8 |
| 15 | -53.8 | -51.3 | 4.0 | 440.1 | 55.5 | -42.0 | 19.2 | 438.5 |
| 16 | -56.2 | -41.5 | 7.0 | 160.5 | 54.0 | -39.0 | 4.8 | 178.6 |
| Ave | -44.4 | -48.8 | 7.0 | 127.5 | 43.1 | -45.3 | 8.7 | 275.5 |

for the influence of motion and form activation patterns on the model. Partial correlations measure the linear relationship between the two conditions after variance shared with all other conditions has been removed (the correlation between the residuals). This approach is beneficial for overcoming similarity relationships that may be masked by common driving inputs from other regions and other shared influences that may be epiphenomenal to the task of interest. Similarity constructed from partial correlation may overcome this limitation by removing shared variance, and retaining only those relationships accounted for uniquely by any two conditions (Salvador et al., 2005; Marrelec et al., 2006). As a result, models of similarity constructed from partial correlations are strongly dependent on the included sources of variance. Our primary partial correlation model included all ten conditions (the three social conditions and their within-scan comparison conditions, plus the two non-social localizers and their controls). Secondary analyses evaluate the impact of including the non-social controls in the full model (Fig. 6) and the similarity structure between only the three primary social conditions (biological motion, faces and social vignettes; Fig. 7).

All spatial pattern analyses were conducted on individual subjects, with the resulting similarity scores Fisher-z transformed and averaged into a single group similarity matrix. The group graphical model consists of nodes - one for each of the conditions - with edges (connections) that reflect the pairwise unique similarity with strength larger than expected by chance. Correlation scores, as shown in the connection thickness scale bars, are converted back to un-transformed r scores (inverse Fisher r-z normalized).

Significance was assessed via permutation tests in which condition labels for each voxel in the activation patterns were randomly swapped (simulating activation patterns drawn from a single distribution). This permutation was implemented on individual subjects, with the resulting individual subject null correlation matrices Fisher-z transformed and then averaged into a single group-level correlation matrix. This permutation process was repeated 10,000 times to generate a null distribution of group similarity coefficients expected by chance. From this distribution we calculated two-tailed 99% confidence intervals and pairwise correlation scores that exceeded these thresholds were deemed statistically significant.

The multiple correlation coefficient is an estimate of the combined influence of two or more variables on the observed variable. Multiple correlations in this multivariate analysis reflect the amount of variance the activation pattern yielded by one condition that can be explained by

Table 2

Multiple correlation scores (model fits) for the partial correlation analysis of the activation patterns, computed separately for the left and right pSTS. Standard deviation (across subjects) are in parentheses.

| Condition | Multiple correlation score per condition | |
|------------|--|-------------|
| | Left pSTS | Right pSTS |
| BioMotion | 0.47 (0.15) | 0.46 (0.14) |
| BioScram | 0.30 (0.15) | 0.27 (0.14) |
| Face | 0.69 (0.10) | 0.73 (0.11) |
| FaceScram | 0.69 (0.10) | 0.72 (0.11) |
| Social | 0.48 (0.15) | 0.44 (0.14) |
| Mechanical | 0.39 (0.13) | 0.32 (0.13) |

the influence of all the other similarity patterns included in the model. Multiple correlation scores for each condition are shown in Table 2.

3. Results

3.1. Mapping the conjunction area

The conjunction pSTS is the region on the posterior extent of the STS with neural activity statistically stronger ($q < 0.05$) during biological motion as compared to scrambled motion, and during face perception as compared to scrambled faces, and when viewing the social animations as compared to the mechanical controls. The conjunction of these three localized activation patterns on the pSTS is shown in Fig. 3 (see also, Table 1). We identified a conjunction pSTS in the left hemisphere of all 16 subjects and in the right hemisphere of 15 subjects.

3.2. Multivariate pattern analysis

Using independent data from the conjunction analysis, we computed the similarity of the spatial pSTS activation patterns resulting from the social localizers (and the two additional control localizers). Graphical models of these similarity structures for the left and right pSTS are shown in Fig. 4. In these models, the conditions are depicted as a graph node with the similarity between each condition shown as a weighted edge. A positive weighted edge indicates two patterns of activation that are more similar than expected by chance, i.e. the most strongly and weakly activated voxels are the same voxels across the two conditions. Negative weighted edges indicate two patterns of activation in which the voxels that are most strongly activated in one condition are the weakly activated voxels in the second condition, and vice versa.

The patterns of activation in the pSTS revealed localizer contrasts (for example, faces and scrambled faces) to be very effective in driving opposing patterns of activation on the pSTS. For all three localizers tested, the pairs of conditions included in the canonical localizers generated patterns of activation that were inversely correlated. Within the pSTS, those voxels most strongly activated during biological motion, face perception and social vignettes were among the most weakly activated by scrambled motion, scrambled faces and mechanical vignettes, respectively.

Moreover, the three social conditions generated similar patterns of activation that were distinctly dissimilar than the localizer control conditions, which themselves shared similarity. Biological motion, face perception and social vignettes are significantly and positively correlated, indicating similarity between the patterns. Likewise, scrambled motion, scrambled faces and mechanical vignettes were significantly positively correlated with each other, albeit more weakly than observed for the social conditions. Together these two patterns of activation reflect two states of the pSTS that are inversely related: that which reflects the encoding of social properties of a stimulus and that which reflects perceptual encoding of non-social features.

Finally, we found that the social conditions each shared some

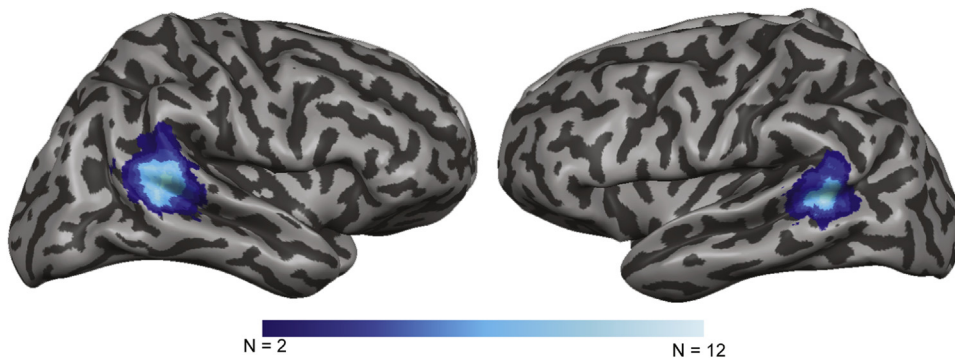


Fig. 3. A count map of the pSTS conjunction regions, computed individually in each of the sixteen subjects using a formal conjunction analysis, and displayed on the anatomy from a single subject. The conjunction analysis identifies voxels in individual subjects that reach statistical significance for each of the three social localizers. There is significant overlap between the identified regions, Talairach coordinates for which are shown in Table 1.

unique variance specific to the pairwise comparisons. Biological motion and face perception share a common activation on the pSTS that is unique from biological motion and social animations, and face perception and social animations generate patterns of activation that are similar and unique from biological motion. Because the partial correlation approach removes the influence of factors that are also present in the control conditions (optic flow and object recognition), we do not attribute the similarity structures to the presence of specific form or motion features.

3.3. Modeling similarity structure outside of the conjunction pSTS

In an exploratory analysis, we considered whether the similarity structure we identified across these conditions was specific to the strict conjunction region on the pSTS. To assess this, we partitioned the STS into seven 10 mm³ segments along the anterior-posterior extent of the sulcus. The segmentation was constructed manually on the individual subject anatomical images such that center segment always aligned with the centroid position for the individual subject's conjunction area. At the extremes, the segments extended well posterior and anterior to the conjunction area. The timeseries for the voxels within each segment were then subjected to the same multivariate similarity analysis as in our primary analysis, using data from only the independent scans that did not contribute to the original mapping of the centroid conjunction area.

We found that the similarity structure depended on location within the sulcus, with the conjunction pSTS positioned at the transition from two distinct similarity profiles (Fig. 5; main effect of subregion: $F(6, 12) = 3.78, p < .01$). Patterns of activation for the three conditions were most similar at and just posterior to the conjunction area, likely reflecting to the strong overlap for localized pSTS observed in this and previous studies (Grossman et al., 2000; Gobbin et al., 2007; Lahnakoski et al., 2012; Engell and McCarthy, 2013). Posterior to the pSTS conjunction area, only the activation patterns for the biological motion and face conditions retained similarity, which decreased precipitously in the more anterior segments. In contrast, activation patterns for biological motion and social vignettes were most similar at and

anterior to the conjunction pSTS. Finally, similarity between activation for face perception and the social vignettes was limited to the conjunction pSTS.

3.4. Additional observations

The multivariate pattern analysis of the conjunction area revealed a few notable post-hoc observations. First, we observed strong (negative) correlations in the activation patterns generated by the experimental and control conditions (i.e. biological motion versus scrambled, faces versus scrambled faces, and social vs mechanical vignettes; as shown in Fig. 4). This inverse relationship is, in part, what makes the pairs of conditions in the social localizers so effective for isolating regions of interest on the pSTS.

Interestingly, we also observed a negative correlation between the spatial patterns elicited by the nonsocial conditions (objects versus scrambled objects, and optic flow versus stationary dots; observed when these conditions were included in a full partial correlation model; Fig. 6A). This was true even though the control conditions elicited weak univariate responses (Fig. 6B). That statistical regularities between the spatial patterns in the pSTS were evident also in the nonsocial conditions was unexpected due to the presumed specialization of pSTS for social features. It is clear, however, that there is some structured information in the pSTS pattern response that discriminates nonsocial visual events, even when those events only weakly activate the region as a whole. This is an interesting finding on its own, but also has relevance to the next point.

A second unexpected observation was the dependence of the similarity structure on the nonsocial control conditions. A model of similarity that is constructed from only the three key social conditions (biological motion, face perception and social vignettes) returns no significant similarity between the pSTS activation patterns for face perception and social vignettes (Fig. 7). The similarity between activation patterns observed between face perception and the social vignettes, which exists only at the conjunction pSTS, also only reaches statistical significance when variance associated with the control conditions is removed (scrambled motion, scrambled faces and mechanical

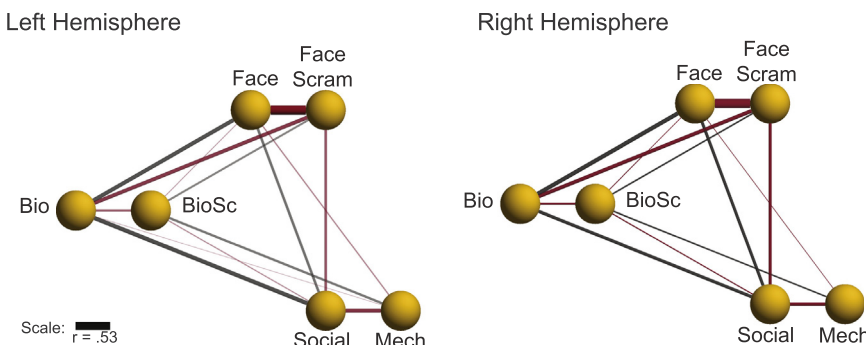
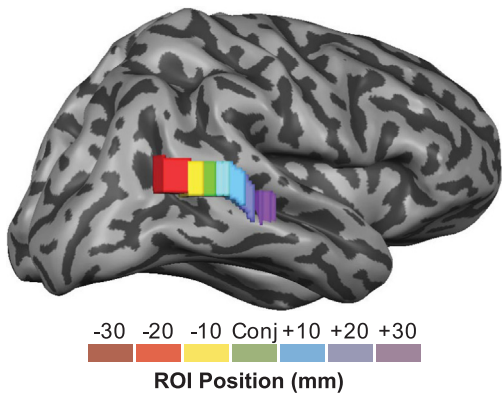


Fig. 4. Graphical model of group results showing the similarity structure constructed from partial correlations using the three social conditions and their localizer controls, after controlling for the effects of the object and motion localizers. Positive correlations are depicted as black lines and negative similarity scores are depicted as red lines. Line thickness and opacity denotes the strength of the similarity score. Only connections significantly stronger than anticipated by chance are shown (see methods).

A. Parcellation of right pSTS



B. Similarity by subregion

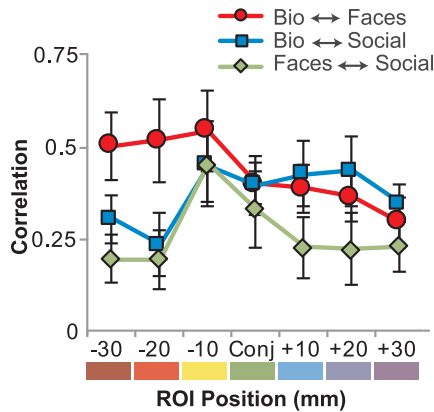


Fig. 5. Similarity scores between the three key social conditions computed separately within anterior-posterior subregions of the STS. (A) A single subject example of the 10 mm³ segments constructed for the right hemisphere STS. The center segment was always positioned at the centroid of the individual subject conjunction area. The anterior and posterior segments were centered in 10 mm increments away from the conjunction centroid, following the topography of the individual subject STS anatomy. (B) Similarity scores from the STS subregions for three key edges: biological motion and faces (red, circles), biological motion and social animations (blue, squares), and faces and social animations (green, diamonds). Error bars depict individual subject variance, ± 1 standard error from the mean. (For interpretation of the

references to color in this figure legend, the reader is referred to the web version of this article.)

vignettes). Similarity structure generated from partial correlations are model-dependent, with the potential to unmask connections otherwise obscured by common driving inputs and spatially distributed sources (Marrelec et al., 2006). In this analysis, the pSTS residual activation patterns for faces and social vignettes are more similar after removing variance linked to the nonsocial control conditions.

Finally, the pSTS activation patterns generally have stronger connectivity weights (higher similarity scores) in correlations computed without removing shared variance as compared to the partial correlation approach. This likely reflects the spatial scale of the distributed nature of the underlying topography, with different neural populations existing at a sub-voxel scale and therefore resulting in activation patterns with strong overall similarity. Importantly, restructuring the variance to account for redundancies in the raw pSTS response still produces a linear model that is highly predictive of the social condition pattern responses, as quantified by the model fits for each condition (Table 2).

4. Discussion

The purpose of this study was to investigate the structure of the pSTS activation patterns generated by three core social perceptual localizer tasks. The underlying topography of functional specialized modules on the STS has been difficult to characterize, although it is of great interest to theoretical and clinical models of STS function (and

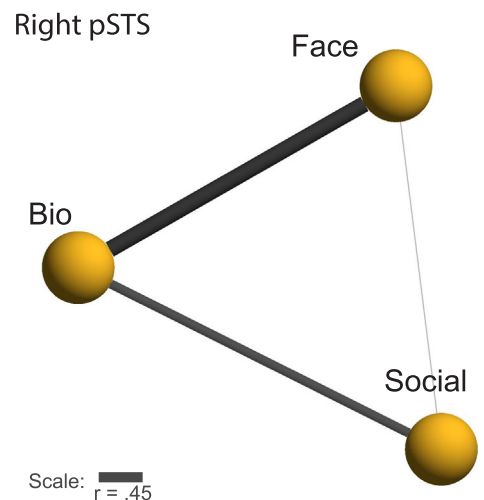
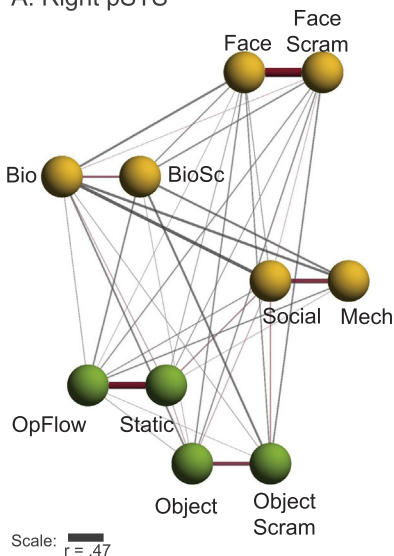


Fig. 7. Similarity model for the right pSTS constructed with only biological motion, face perception and social vignettes (omitting the baseline conditions), illustrating the extremely weak similarity between face perception and the social vignettes.

A. Right pSTS



B. Univariate contrast

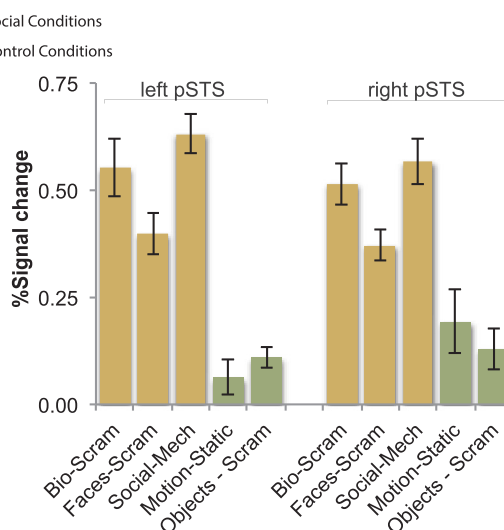


Fig. 6. (A) Similarity model from the right pSTS constructed all localizers (including the non-social localizers) contributing to the full partial correlation model. The negative correlation is apparent between activation patterns generated by the contrasting conditions of each localizer, including the contrasting conditions of each localizer, including the contrasting objects vs scrambled objects, and optic flow vs stationary, conditions. (B) Percent signal change (the univariate effect size) in the left and right pSTS for the five localizers. Social localizers are shown in yellow, the non-social control conditions are shown in green. Error bars indicate ± 1 standard error (between subject variance). (For interpretation of the references to color in this figure legend, the reader is referred to the web version of this article.)

dysfunction) in social perception and cognition. We used a multivariate pattern analysis approach that quantifies the similarity between spatial activation patterns generated by key fMRI localizers that isolate the pSTS, while also considering the influence of redundant variance likely to be reflected in a micro-modular structure (smaller in organization as compared to the voxel size). All of these analyses were conducted on the pSTS isolated using a formal conjunction analysis using actions, faces and social vignettes.

We found a strong, negative correlation in the spatial activation profiles on the pSTS as identified by the social conditions (biological motion, faces and social vignettes) as compared to their respective control conditions. Together these two patterns of activation reflect two states of the pSTS that are inversely related: that which reflects the encoding of social properties of a stimulus and that which reflects perceptual encoding of non-social features.

We also found strong similarity in the statistical structure of the activation patterns unique to each pairwise social comparison. To the extent that partial correlations are effective in controlling for variance common to more than one condition, the similarities in these activation patterns reflect variance unique to biological motion and face perception, face perception and social vignettes, and social vignettes and biological motion.

These similarity relationships also varied across the sulcal topography surrounding the conjunction pSTS. Similarity was strongest between the social conditions in the more posterior aspects of the STS, whereas the variance shared between biological motion and face perception was stronger more anterior on the STS. This evidence for an anterior-posterior topography of functional specificity in the STS is consistent with the notion of a modular organization on the pSTS embedded within complex activation patterns and distinguishable through multivariate approaches (Deen et al., 2015; Isik et al., 2017). Our analyses are evidence supporting multiplexed and higher-order (i.e. not driven by perceptual features) encoding of social cues only within the conjunction pSTS. The distinct patterns of similarity along the STS outside of the conjunction region is also consistent with segregated animacy "detectors" by cue type, as proposed by Shultz et al. (2015). Our data show shared neural populations for the encoding of body parts (i.e. faces and body actions) and implied agency through those features in the more posterior STS, with implied animacy as through motion cues in the more anterior STS.

Our findings underscore the richness of the statistical structure embedded within the voxel-wise BOLD response on the STS. Univariate mapping studies have successfully dissociated biological motion perception and social animations from engaging false-belief tasks, but typically report significant overlap in topography for biological motion and face perception (Grossman et al., 2000; Gobbini et al., 2007; Engell and McCarthy, 2013; Deen et al., 2015). Our results demonstrate that this similarity peaks in the more posterior STS and reflects only one component of many within the multivariate pSTS pattern response.

This information laden statistical structure of the human pSTS is not surprising in the context of the single-unit investigations of the monkey STS_a, the proposed homologous region. These studies describe a heterogeneous population of neurons tuned to the perceptual features of bodies and actions (facial movements, gaze, bodies and actions) and goal-directed information depicted by agents (Perrett et al., 1985a, 1985b; Hasselmo et al., 1989; Wachsmuth et al., 1994; Jellema et al., 2000; Singer and Sheinberg, 2010; Vangeneugden et al., 2011). Such diverse neurons exist intermingled on the monkey STS, with some evidence for patchy organization that is difficult to discern even using fMRI-guided unit penetrations (Popivanov et al., 2014; Nelissen et al., 2011). Thus we must conclude that if specialized function does exist on the human pSTS, as it appears in the monkey STS_a, then it is likely on a spatial scale that is difficult to evaluate using standard univariate mapping approaches. The results from our study are consistent with the patchy organization observed in monkey STS_a, which we would characterize as "micro-modular", in which specialized neural populations

tuned to distinct properties of social cues cluster at a spatial scale finer than that of a typical fMRI mapping study.

Our findings are also consistent with theoretical models of the pSTS in which perceptual units exist tuned to specific body features, with those populations distinct from neurons tuned to motion features that signal animacy (Shultz et al., 2015). Most accounts also propose there to be additional units that decode intentionality and goal-directed inferences (Puce and Perrett, 2003). At least one prominent model proposes a hierarchical structure of neural units with tuning to the perceptual properties of social cues, which serve as the building blocks to scaffolding inferred properties of the events (Jellema and Perrett, 2006). Future research is required to determine a means by which to isolate these two sensory and inferential populations.

We note that a fully integrated "multiplexed" brain region that extracts social cognitive cues from a wide assortment of visual events (such as that proposed by Hein and Knight, 2008) would not have yielded the patterns of similarity that we observed. An integrated model would generate a fully-connected model of similarity as computed from the full correlations, and a completely disconnected model from the partial correlation approach. In other words, the pattern of activation would be shared among all three tasks, and thus partitioned out when removing redundant variance shared among three or more tasks. Our data do not support that model.

Although social perception and cognition are sometimes associated with right hemisphere lateralization, we found only hints of right hemisphere dominance, and little differences in the neural pattern structure between the right and left pSTS. Overall the volumetric extent of the pSTS in the right hemisphere tended to be larger than that identified in the left pSTS, although the univariate BOLD in the social cue conditions was not significant statistically (Fig. 6). We found no significant hemispheric differences in the strength of similarity between our social perception conditions.

This investigation also yielded some additional, unexpected discoveries. For example, we found structure in the variance that reflected similarity in the pattern of responses to conditions for which the pSTS only elicited weak univariate responses. These included the control conditions for the social localizers, and the nonsocial control conditions (optic flow and object recognition). That there is structure in the pattern response for visual events that do not drive maximal BOLD response is not new (Haxby et al., 2001), but to our knowledge this is one of the first demonstrations in the human STS.

Our results show there exists a mixed population of neurons within the conjunction pSTS, some of which reflect non-social components of the localizer. These neural responses to nonsocial features obscure the underlying shared statistical structure at the conjunction pSTS despite the relatively weak univariate BOLD activation levels. These structured, but uncorrelated, activation patterns exist intermixed with the neural responses to the social conditions. Further analyses are required to better understand the nature of these responses, but we hypothesize they may reflect the perceptual encoding of visual features, which vary dramatically between these localizers but are well controlled by the baseline conditions.

The implication of these results have broader significance in the study of autism, a neurodevelopmental disorder of social communication linked to atypical structural and functional connectivity of the posterior STS (Gligal et al., 2014; Pavlova, 2012; Zilbovicius et al., 2006). A hallmark of social behavior autism is the difficulty in making spontaneous inferences as to the mental states of others (Baron-Cohen et al., 1985), which in turn is believed to reflect impairments in the earlier development of receptive and self-initiated shared and joint attention (Mundy and Newell, 2007). Shared and joint attention in social interactions develops very early, within the first year or so of life, and relies heavily on the use and evaluation of social cues such as eye gaze and pointing (Carpenter et al., 1998). Attention to these cues is diminished in autism, evident in gaze patterns in infants and children (Frazier et al., 2017; Klin et al., 2009). Our results indicate that the

topography of functional selectivity along the STS may promote the differentiated decoding of social cues based on their perceptual features. Disorganization of connectivity in the STS, either through reduced local pruning or via decreased integrity of long-range white matter tracts, may therefore impair the efficacy by which the neural signals associated with these social cues can be distinguished and interpreted reliably. Together, the micro-modular organization of the pSTS with altered connectivity may promote significant vulnerabilities in the neural transmission of socially relevant cues to the large social cognitive brain networks.

Acknowledgments

This material is based on work supported by the National Science Foundation under NSF BCS0748314 awarded to E. Grossman. We thank Alex Martin for sharing his social and mechanical vignette stimuli for use in this study.

References

- Bahnemann, M., Dziobek, I., Prehn, K., Wolf, I., Heekeren, H.R., 2010. Sociotopy in the temporoparietal cortex: common versus distinct processes. *Social. Cogn. Affect. Neurosci.* 5, 48–58.
- Baron-Cohen, S., Leslie, A.M., Frith, U., 1985. Does the autistic child have a "theory of mind"? *Cognition* 21, 37–46.
- Beauchamp, M.S., Lee, K.E., Haxby, J.V., Martin, A., 2002. Parallel visual motion processing streams for manipulable objects and human movements. *Neuron* 34 (1), 149–159.
- Brainard, D.H., 1997. The psychophysics toolbox. *Spat. Vis.* 10 (4), 433–436.
- Carpenter, M., Nagell, K., Tomasello, M., Butterworth, G., Moore, C., 1998. Social cognition, joint attention, and communicative competence from 9 to 15 months of age. *Monogr. Soc. Res. Child Dev.* 63, i-174.
- Carter, R.M., Huettel, S.A., 2013. A nexus model of the temporal–parietal junction. *Trends Cogn. Sci.* 17 (7), 328–336.
- Castelli, F., Happé, F., Frith, U., Frith, C., 2000. Movement and mind: a functional imaging study of perception and interpretation of complex intentional movement patterns. *Neuroimage* 12 (3), 314–325.
- Deen, B., Koldewyn, K., Kanwisher, N., Saxe, R., 2015. Functional organization of social perception and cognition in the superior temporal sulcus. *Cereb. Cortex* 25 (11), 4596–4609.
- Dziura, S.L., Thompson, J.C., 2014. Social-network complexity in humans is associated with the neural response to social information. *Psychol. Sci.* 25 (11), 2095–2101.
- Engell, A.D., McCarthy, G., 2013. Probabilistic atlases for face and biological motion perception: an analysis of their reliability and overlap. *Neuroimage* 74, 140–151.
- Frazier, T.W., Strauss, M., Klingemier, E.W., Zetzer, E.E., Hardan, A.Y., 2017. A meta-analysis of gaze differences to social and nonsocial information between individuals with and without autism. *J. Am. Acad. Child Adolescent Psychiatry* 56, 546–555.
- Gallagher, H.L., Frith, C.D., 2003. Functional imaging of 'theory of mind'. *Trends Cogn. Sci.* 7 (2), 77–83.
- Gao, T., Scholl, B.J., McCarthy, G., 2012. Dissociating the detection of intentionality from animacy in the right posterior superior temporal sulcus. *J. Neurosci.* 3241, 14276–14280.
- Genovese, C.R., Lazar, N.A., Nichols, T., 2002. Thresholding of statistical maps in functional neuroimaging data using the false discovery rate. *Neuroimage* 15 (4), 870–878.
- Gligal, T., Jones, E.J.H., Bedford, R., Charman, T., Johnson, M.H., 2014. From early markers to neurodevelopmental mechanisms of autism. *Dev. Sci.* 34, 189–207.
- Gobbini, M.I., Koralek, A.C., Bryan, R.E., Montgomery, K.J., Haxby, J.V., 2007. Two takes on the social brain: a comparison of theory of mind tasks. *J. Cogn. Neurosci.* 19 (11), 1803–1814.
- Grosbras, M.H., Beaton, S., Eickhoff, S.B., 2012. Brain regions involved in human movement perception: a quantitative voxel-based meta-analysis. *Hum. Brain Mapp.* 33 (2), 431–454.
- Grossman, E., Donnelly, M., Price, R., Pickens, D., Morgan, V., Neighbor, G., Blake, R., 2000. Brain areas involved in perception of biological motion. *J. Cogn. Neurosci.* 12 (5), 711–720.
- Grossman, E.D., Blake, R., 2002. Brain areas active during visual perception of biological motion. *Neuron* 35 (6), 1167–1175.
- Hasselmo, M.E., Rolls, E.T., Baylis, G.C., Nalwa, V., 1989. Object-centered encoding by face-selective neurons in the cortex in the superior temporal sulcus of the monkey. *Exp. Brain Res.* 75 (2), 417–429.
- Haxby, J.V., Gobbini, M.I., Furey, M.L., Ishai, A., Schouten, J.L., Pietrini, P., 2001. Distributed and overlapping representations of faces and objects in ventral temporal cortex. *Science* 293 (5539), 2425–2430.
- Haxby, J.V., Hoffman, E.A., Gobbini, M.I., 2000. The distributed human neural system for face perception. *Trends Cogn. Sci.* 4 (6), 223–233.
- Hoffman, E.A., Haxby, J.V., 2000. Distinct representations of eye gaze and identity in the distributed human neural system for face perception. *Nat. Neurosci.* 3 (1), 80–84.
- Heider, F., Simmel, M., 1944. An experimental study of apparent behavior. *Am. J. Psychol.* 57 (2), 243–259.
- Hein, G., Knight, R.T., 2008. Superior temporal sulcus - it's my area: or is it? *J. Cogn. Neurosci.* 20 (12), 2125–2136.
- Isik, L., Koldewyn, K., Beeler, D., Kanwisher, N., 2017. Perceiving social interactions in the posterior superior temporal sulcus. *Proc. Natl. Acad. Sci.* <https://doi.org/10.1073/pnas.1714471114>.
- Klin, A., Lin, D.J., Gorrindo, P., Ramsay, G., Jones, W., 2009. Two-year-olds with autism orient to nonsocial contingencies rather than to biological motion. *Nature* 459, 257.
- Jastorff, J., Orban, G.A., 2009. Human functional magnetic resonance imaging reveals separation and integration of shape and motion cues in biological motion processing. *J. Neurosci.* 29 (22), 7315–7329.
- Jellema, T., Baker, C.I., Wicker, B., Perrett, D.I., 2000. Neural representation for the perception of the intentionality of actions. *Brain Cogn.* 44 (2), 280–302.
- Jellema, T., Perrett, D.I., 2006. Neural representations of perceived bodily actions using a categorical frame of reference. *Neuropsychologia* 44 (9), 1535–1546.
- Lahnakoski, J.M., Glerean, E., Salmi, J., Jääskeläinen, I.P., Sams, M., Hari, R., Nummenmaa, L., 2012. Naturalistic fMRI mapping reveals superior temporal sulcus as the hub for the distributed brain network for social perception. *Front. Hum. Neurosci.* 6. <https://doi.org/10.3389/fnhum.2012.00233>.
- Langner, O., Dotsch, R., Bijlstra, G., Wigboldus, D.H., Hawk, S.T., van Knippenberg, A., 2010. Presentation and validation of the radboud faces database. *Cogn. Emot.* 24 (8), 1377–1388.
- Lee, S.M., McCarthy, G., 2014. Functional heterogeneity and convergence in the right temporoparietal junction. *Cereb. Cortex* 26 (3), 1108–1116.
- Marrelec, G., Krainik, A., Duffau, H., Péligrini-Issac, M., Lehericy, S., Doyon, J., Benali, H., 2006. Partial correlation for functional brain interactivity investigation in functional MRI. *Neuroimage* 32 (1), 228–237.
- Martin, A., Weisberg, J., 2003. Neural foundations for understanding social and mechanical concepts. *Cogn. Neuropsychol.* 20 (3–6), 575–587.
- Morrone, M.C., Tosetti, M., Montanaro, D., Fiorentini, A., Cioni, G., Burr, D.C., 2000. A cortical area that responds specifically to optic flow, revealed by fMRI. *Nat. Neurosci.* 3 (12), 1322–1328.
- Mundy, P., Newell, L., 2007. Attention, joint attention and social cognition. *Curr. Direct. Psychol. Sci.* 16, 269–274.
- Nelissen, K., Borra, E., Gerbella, M., Rozzi, S., Luppino, G., Vanduffel, W., Rizzolatti, G., Orban, G.A., 2011. Action Observation circuits in the Macaque monkey. *Cortex* 31 (10), 3743–3756.
- Nichols, T., Brett, M., Andersson, J., Wager, T., Poline, J.-B., 2005. Valid conjunction inference with the minimum statistic. *Neuroimage* 25 (3), 653–660.
- Pavlova, M.A., 2012. Biological motion processing as a hallmark of social cognition. *Cereb. Cortex* 22, 981995.
- Pelli, D.G., 1997. The VideoToolbox software for visual psychophysics: transforming numbers into movies. *Spat. Vis.* 10 (4), 437–442.
- Perrett, D.I., Smith, P.A., Mistlin, A.J., Chitty, A.J., Head, A.S., Potter, D.D., Broennimann, R., Milner, A.D., Jeeves, M.A., 1985a. Visual analysis of body movements by neurons in the temporal cortex of the macaque monkey: a preliminary report. *Behav. Brain Res.* 16 (2), 153–170.
- Perrett, D.I., Smith, P.A.J., Potter, D.D., Mistlin, A.J., Head, A.S., Milner, A.D., Jeeves, M.A., 1985b. Visual cells in the temporal cortex sensitive to face view and gaze direction. *Proc. R. Soc. Lond. B: Biol. Sci.* 223 (1232), 293–317.
- Popivanov, I.D., Jastorff, J., Vanduffel, W., Vogels, R., 2014. Heterogeneous single-unit selectivity in an fMRI-defined body-selective patch. *J. Neurosci.* 34 (1), 95–111.
- Puce, A., Allison, T., Bentin, S., Gore, J.C., McCarthy, G., 1998. Temporal cortex activation in humans viewing eye and mouth movements. *J. Neurosci.* 18 (6), 2188–2199.
- Puce, A., Perrett, D., 2003. Electrophysiology and brain imaging of biological motion. *Philos. Trans. R. Soc. Lond. B: Biol. Sci.* 358 (1431), 435–445.
- Pyles, J.A., Grossman, E.D., 2013. Neural mechanisms for biological motion and animacy. In: Shiffrar, M., Johnson, K. (Eds.), *People Watching: Social, Perceptual and Neurophysiological Studies of Body Perception*. Oxford University Press.
- Salvador, R., Suckling, J., Coleman, M.R., Pickard, J.D., Menon, D., Bullmore, E.D., 2005. Neurophysiological architecture of functional magnetic resonance images of human brain. *Cereb. Cortex* 15, 1332–1342.
- Saxe, R., Wexler, A., 2005. Making sense of another mind: the role of the right temporoparietal junction. *Neuropsychologia* 43(10), 1391–1399.
- Saxe, R., Whitfield-Gabrieli, S., Scholz, J., Pelphrey, K.A., 2009. Brain regions for perceiving and reasoning about other people in school-aged children. *Child Dev.* 80(4), 1197–1209.
- Shultz, S., Honert, R., Engell, A.D., McCarthy, G., 2015. Stimulus-induced reversal of information flow through a cortical network for animacy perception. *Soc. Cogn. Affect. Neurosci.* 10(1), 129–135.
- Singer, J.M., Sheinberg, D.L., 2010. Temporal cortex neurons encode articulated actions as slow sequences of integrated poses. *J. Neurosci.* 30 (8), 3133–3145.
- Van Overwalle, F., 2009. Social cognition and the brain: a meta-analysis. *Hum. Brain Mapp.* 30 (3), 829–858.
- Wachsmuth, E., Oram, M.W., Perrett, D.I., 1994. Recognition of objects and their component parts: responses of single units in the temporal cortex of the macaque. *Cereb. Cortex* 4 (5), 509–522.
- Vangeneugden, J., De Maziere, P.A., Van Hulle, M.M., Jaeggli, T., Van Gool, L., Vogels, R., 2011. Distinct mechanisms for coding of visual actions in macaque temporal cortex. *J. Neurosci.* 31 (2), 385–401.
- Xia, M., Wang, He, Y., 2013. BrainNet viewer: a network visualization tool for human brain connectomics. *PLoS ONE* 8 (7), e689. <https://doi.org/10.1371/journal.pone.0068910>.
- Yang, D.Y.-J., Rosenblau, G., Keifer, C., Pelphrey, K.A., 2015. An integrative neural model of social perception, action observation and theory of mind. *Neurosci. Biobehav. Rev.* 51, 263–275.
- Zilbovicius, M., Meresse, I., Chabane, N., Brunelle, F., Samson, Y., Boddaert, N., 2006. Autism, the superior temporal sulcus and social perception. *Trends Neurosci.* 29, 359–366.